



Controlled epi-cortical delivery of epidermal growth factor for the stimulation of endogenous neural stem cell proliferation in stroke-injured brain

Michael J. Cooke^{a,1}, Yuanfei Wang^{a,b,1}, Cindi M. Morshead^{b,c}, Molly S. Shoichet^{a,b,d,*}

^a Department of Chemical Engineering and Applied Chemistry, University of Toronto, 200 College Street, Toronto, ON, Canada M5S 3E5

^b Institute of Biomaterials and Biomedical Engineering, 164 College Street, Room 407, Toronto, ON, Canada M5S 3G9

^c Department of Surgery, University of Toronto, 160 College Street, Room 1006, Toronto, ON, Canada M5S 3E1

^d Department of Chemistry, University of Toronto, 80 St. George Street, Toronto, ON, Canada M5S 3H6

ARTICLE INFO

Article history:

Received 25 March 2011

Accepted 12 April 2011

Available online 7 May 2011

Keywords:

Hydrogel

Stroke

Epidermal growth factor

Tissue penetration

Poly(ethylene glycol)

Drug delivery

ABSTRACT

One of the challenges in treating central nervous system (CNS) disorders with biomolecules is achieving local delivery while minimizing invasiveness. For the treatment of stroke, stimulation of endogenous neural stem/progenitor cells (NSPCs) by growth factors is a promising strategy for tissue regeneration. Epidermal growth factor (EGF) enhances proliferation of endogenous NSPCs in the subventricular zone (SVZ) when delivered directly to the ventricles of the brain; however, this strategy is highly invasive. We designed a biomaterials-based strategy to deliver molecules directly to the brain without tissue damage. EGF or poly(ethylene glycol)-modified EGF (PEG-EGF) was dispersed in a hyaluronan and methylcellulose (HAMC) hydrogel and placed epi-cortically on both uninjured and stroke-injured mouse brains. PEG-modification decreased the rate of EGF degradation by proteases, leading to a significant increase in protein accumulation at greater tissue depths than previously shown. Consequently, EGF and PEG-EGF increased NSPC proliferation in uninjured and stroke-injured brains; and in stroke-injured brains, PEG-EGF significantly increased NSPC stimulation. Our epi-cortical delivery system is a minimally-invasive method for local delivery to the brain, providing a new paradigm for local delivery to the brain.

© 2011 Elsevier Ltd. All rights reserved.

1. Introduction

Effective treatment of central nervous system (CNS) disorders, including those of the brain and the spinal cord, remain highly challenging today. This is partly due to the difficulties associated with delivering drugs to the CNS in a controlled and minimally-invasive manner. Local delivery is currently achieved using a catheter/minipump system; however, prolonged use of this invasive system carries risks of infection [1–3]. Alternative strategies, such as systemic delivery, are limited by the blood–brain barrier (BBB), which prevents most systemically administered drugs from penetrating into the brain [4,5]. While some molecules can cross the BBB, systemic administration of a high dose is required to achieve therapeutic levels in the brain, thus resulting in undesired systemic side effects. There is significant need for a delivery strategy that enables local, sustained release to the brain without tissue damage. A biomaterials-based strategy offers the potential to meet this challenge.

Stroke is currently the third leading cause of death in the industrialized world, leading to 15 million injuries and 5 million deaths each year [6]. Stroke results from the occlusion or rupture of cerebral arteries. While there is currently no effective treatment for stroke, tissue regeneration by endogenous stem cell stimulation holds promise for functional repair [7,8]. This neuroregenerative approach may be facilitated by delivering growth factors to stimulate proliferation of endogenous stem cells in the brain. The neural stem cell niche in the subventricular zone (SVZ) is located along the walls of the lateral ventricles of the brain [9–11]. Following stroke, neural stem/progenitor cells (NSPCs) in the SVZ are stimulated to proliferate, but at insufficient levels to regenerate damaged tissue [12,13]. Therapeutic factors infused into the ventricles of the brain promote endogenous stem cell activation, as has been shown with numerous factors, including: epidermal growth factor (EGF) [7,14]; erythropoietin (EPO) [7]; nerve growth factor (NGF) [15]; cyclosporine A [8]; colony stimulating factor (CSF) [16]; and basic fibroblast growth factor (bFGF) [15]. Recombinant EGF administered into the cerebroventricles via an osmotic minipump system enhances the proliferation of endogenous NSPCs in the SVZ [7], but prolonged use of the osmotic minipump system damages brain tissue.

* Corresponding author. Department of Chemical Engineering and Applied Chemistry, University of Toronto, 200 College Street, Toronto, ON, Canada M5S 3E5.

E-mail address: molly.shoichet@utoronto.ca (M.S. Shoichet).

¹ Both authors are equally contributed as joint first authors.

With the aim of designing a minimally-invasive system for sustained drug release to the brain, we developed a polymeric drug delivery vehicle comprised of a physical blend of hyaluronan (HA) and methylcellulose (MC), termed HAMC. It is an injectable, shear thinning hydrogel that is inversely thermal gelling, with MC forming hydrophobic physical crosslinks at reduced temperature due to the presence of HA, while retaining its ability to flow due to the shear thinning property of HA [17]. HAMC gels upon injection into physiological environments, such as the intrathecal space surrounding the spinal cord, where local release has been achieved [18]. To design a minimally-invasive strategy to deliver molecules directly to brain tissue, we examined the use of HAMC for local delivery to the brain and evaluated whether remote delivery of EGF would stimulate the endogenous stem cells in the SVZ that are critical for self-repair after stroke.

To achieve local delivery to the brain, without injection directly into brain tissue, EGF was incorporated in HAMC and deposited directly on the cortex surface. By spatially confining HAMC within a custom-designed casing on top of the cortex (Fig. 1), the feasibility of remote delivery of EGF to the SVZ target tissue was examined. While this strategy is less invasive than direct injection into the ventricles of the brain, it was not known whether remote delivery would result in sufficient tissue penetration of EGF to reach the SVZ. Diffusion of proteins in brain tissue is primarily dependent on intrinsic diffusivity of the protein, tissue tortuosity, and protein elimination from the diffusion path. A combination of these factors limits protein diffusion distance in the brain to 1–2 mm [19]; however, the SVZ resides approximately 2.5–3 mm below the cortical surface [20]. Thus the penetration distance of EGF is likely inadequate to reach the SVZ, thus severely impeding the development of an epi-cortical delivery system. Importantly, N-terminal modification of EGF with 5 kDa poly(ethylene glycol) (PEG) increases the *in vivo* diffusion distance following bolus injection [21].

Here we investigated the penetration distance of EGF and mono-PEG-modified EGF (PEG-EGF) in uninjured and stroke-injured

mouse brains following epi-cortical delivery from HAMC. To gain insight into the mechanism accounting for differences in tissue penetration, brain extracts were examined for proteolytic degradation. We also studied the effect of PEG-modification on the degradation of EGF in the brain. Furthermore we investigated the potential of using HAMC as a vehicle for epi-cortical drug delivery to the brain, and the possibility of using PEG-modification to enhance the tissue penetration of remotely delivered proteins to stimulate endogenous neural stem cells in the brain.

2. Materials and methods

2.1. Materials

1.4–1.8 × 10⁶ g/mol sodium hyaluronan (HA) was purchased from NovaMatrix (Sandvika, Norway). 3.4 × 10⁵ g/mol methylcellulose (MC) was obtained from Shin Etsu (Chiyoda-ku, Tokyo, Japan). Recombinant human epidermal growth factor (EGF) and the EGF ELISA detection kit were purchased from PeptoTech Inc. (Rocky Hill, NJ, USA). Methoxy-poly(ethylene glycol, 5 kDa) activated with propionaldehyde (mPEG-PPA) was purchased from NOF Corp. (Tokyo, Japan). Mouse anti-human Ki-67 and mouse anti-rat nestin were purchased from BD biosciences (Mississauga, ON, Canada), mouse anti-rat GFAP was obtained from Millipore Inc. (Billerica, MA, USA), rabbit anti-mouse Ki-67 and rabbit anti-mouse double-cortin were obtained from Abcam (Cambridge, MA, USA), and Vectashield with DAPI stain was purchased from Vectorlabs (Burlington, ON, Canada). Alexa 488 and Alexa 564 goat-anti-rabbit IgG, and Alexa 488 and Alexa 568 goat-anti-mouse IgG were obtained from Invitrogen Inc. (Burlington, ON, Canada). Sodium cyanoborohydride (NaCNBH₃), NaCl, MgCl₂, CaCl₂, BaCl₂, Na₂HPO₃, NaH₂PO₃ TES, MES, ethylenediamine tetraacetic acid (EDTA), ethylene glycol-bis(2-aminoethyl)-N,N,N',N'-tetraacetic acid (EGTA), phenylmethanesulfonyl fluoride (PMSF), dithiothreitol, sodium acetate buffer salts, and protease inhibitor panel were supplied by Sigma–Aldrich (Oakville, ON, Canada). Artificial cerebrospinal fluid (aCSF [21]) and all buffers were prepared with distilled and deionized water prepared from a Millipore Milli-RO 10 Plus and Milli-Q UF Plus at 18 MΩ m resistivity (Millipore, Bedford, USA). MicroBCA protein assay kit was obtained from Thermo Fisher Scientific (Rockford IL, USA) and used as per the manufactures instructions.

2.2. Preparation of sterile HAMC

HA and MC were dissolved in dH₂O, sterile-filtered and lyophilized under sterile conditions. The resulting sterile polymers were kept at 4 °C until use. HAMC was

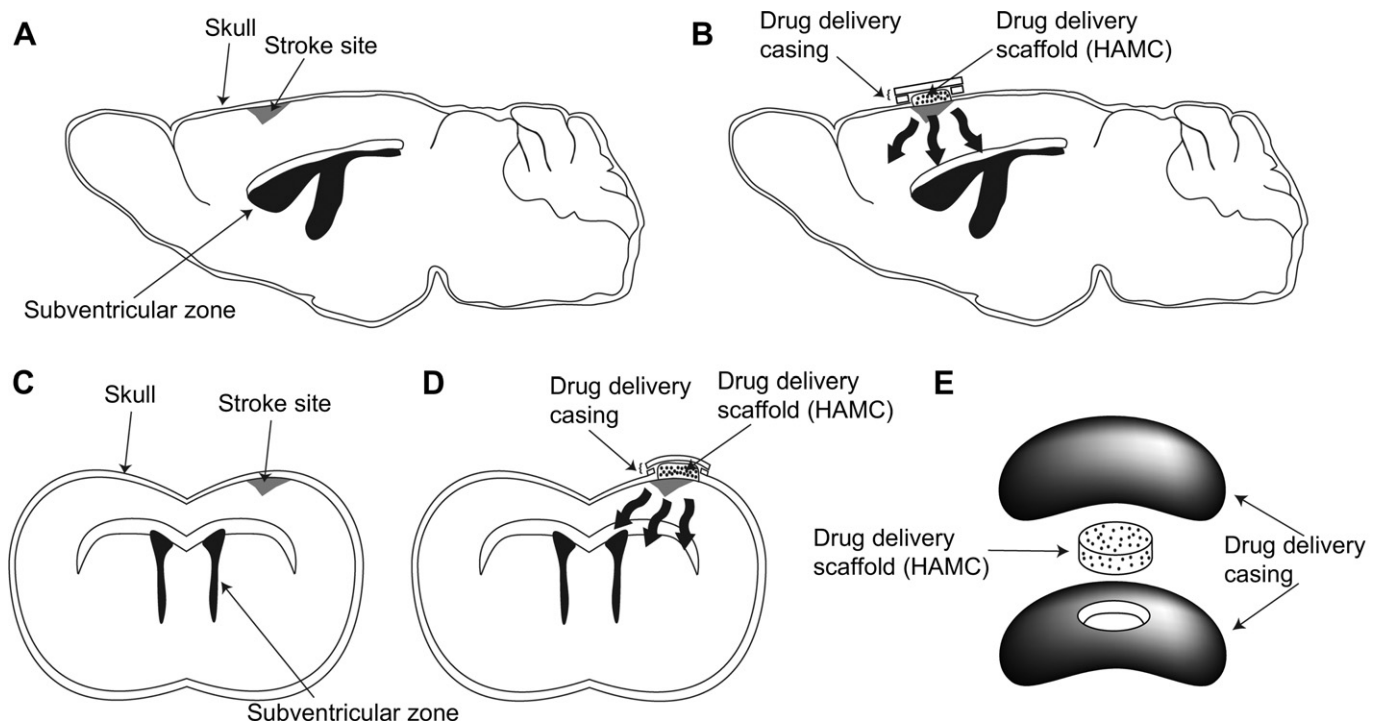


Fig. 1. Schematic for localized and sustained delivery of drugs to the brain. (A) Sagittal view of stroke-injured mouse brain with (B) drug delivery system. (C) Coronal view of stroke-injured mouse brain with (D) drug delivery system. (E) Drug delivery system in expanded view.

produced with 1 w/v% HA and 2 w/v% MC dissolved in sterile aCSF, mixed using a Speed Mixer DAC 150 FVZ (Siemens) and centrifuged to remove air bubbles. Subsequently, 10 μ l of 1.6 mM solutions of EGF or PEG-EGF was added to 900 μ l HAMC, mixed and centrifuged to eliminate air bubbles.

2.3. *In vitro* release of EGF and PEG-EGF from HAMC

To estimate the time required for EGF and PEG-EGF to diffuse from the HAMC implant *in vivo*, we studied their release from HAMC *in vitro*. 100 μ l of HAMC containing 0.16 mM of either EGF or PEG-EGF was injected into the bottom of a 2 ml eppendorf tube and allowed to gel for 20 min at 37 °C. 900 μ l of aCSF was incubated to 37 °C and slowly added to the gel. The supernatant was removed at each time point and replaced with fresh aCSF. The amount of protein released was analysed at $t = 0, 15, 30$ min, 1, 2, 3, 4, 5, 6, 8, 12, 24 h. The cumulative amount released at each time point was plotted against time.

2.4. Mouse surgeries

All experiments were carried out in accordance with the Guide to the Care and Use of Experimental Animals developed by the Canadian Council on Animal Care and approved by the Animal Care Committee at the University of Toronto. All animals used in this study were 9–11 week old C57BL/6 mice (Charles River, QC, Canada). A total of 75 animals were used in these studies.

Stroke surgeries were carried out as described by Tennant et al. [22]. Mice were anaesthetised with isoflurane, shaved and placed into a Kopf stereotaxic instrument. A midline incision in the scalp was made. A small burr hole was made in the skull at the coordinates 2.25 lateral to the midline and 0.6 anterior to the Bregma. Using a 26 G needle, the vasoconstrictor endothelin-1 (400 pM, Calbiochem, Gibbstown, NJ, USA) was injected 1.0 ventral to the surface of the brain at a rate of 0.1 μ l/min with a total volume of 1.0 μ l. The needle was left in place for 10 min prior to removal. The incision was sutured, antibiotic ointment applied and the animal was allowed to recover under a heat lamp.

2.5. Preparation of delivery device for HAMC implantation

HAMC was contained on the cortex of the brain in a custom-made device. The device consists of two polycarbonate disks (0.5 mm height \times 5.9 mm outside diameter). The central opening of one spacer was enlarged to 2 mm in diameter. The second spacer was unmodified. Both spacers were slightly heated and moulded into a concave shape to match the curvature of the skull (Fig. 1). The spacers were sterilized with ethylene oxide prior to use.

2.6. Drug delivery device implantation surgeries

Uninjured mice were anaesthetised with isoflurane, shaved and placed into a Kopf stereotaxic instrument. A midline incision in the scalp was made. A small burr hole was made in the skull at the coordinates 2.25 lateral to the midline and 0.6 anterior to Bregma. The exposed dura was pierced using a 26 G needle. A spacer with 2 mm opening was fixed over the burr hole with bone glue. 3 μ l of either HAMC alone or HAMC with growth factor was placed into the central opening in direct contact with the brain cortical surface. A second spacer without an opening was placed above the first spacer and fixed with bone glue. The skin was sutured over the spacer system.

For mice with stroke surgeries, the drug delivery implant was inserted at day 4 post stroke. The sutures were removed to expose the burr hole and any tissue debris was removed using a 26 G needle. HAMC or HAMC with growth factor was implanted as above. The animal was re-sutured after implantation.

2.7. Analysis of *in vivo* protein penetration

Animals were sacrificed at 2 h, 6 h, 1 day, and 2 days post-implantation. The spacers containing HAMC were removed from the skull and placed into a 2 ml eppendorf tube and 0.5 ml of ELISA diluents solution (0.1% Tween 20 in 150 mM PBS) was added. The tube was kept on a rotary shaker at 4 °C overnight to extract any growth factors remaining in the gel.

Brains were extracted and snap frozen using CO₂(s) cooled isopropane and stored at –80 °C. Three 1 mm coronal slices were prepared, at the injection site and rostral and caudal to the injection site. Coronal slices were prepared using McIlwain tissue chopper (790744-11, Mickle laboratory engineering company, Surrey, UK). Dorsal-ventral sections (0.5 mm) were then obtained from each coronal slice using Leica CM3050S cryostat system operating at –18 °C. Each 0.5 mm section was transferred into 2 ml polystyrene microtubes (Sarstedt 72.694.006, Montreal, Quebec, Canada) and 200 μ l homogenizing buffer (20 mM HEPES, 10 mM KCl, 1.5 mM MgCl₂, 1 mM EDTA, 1 mM EGTA, 1 mM dithiothreitol, 1 mM PMSF) was added to each tube. Tissue sections were homogenized with 1.0 mm diameter zirconia beads. To remove tissue fragments, homogenized tissue was centrifuged at 15,000 RPM for 15 min at 4 °C and the homogenate was transferred into 1.75 ml eppendorf tubes. 200 μ l ELISA diluent solution was used to dilute homogenate to a total volume of 400 μ l.

The amount of protein remaining in the gel and in the brain homogenate at each time point were analysed by EGF ELISA (PeproTech) as per the manufacturer's instructions. The amount of protein remaining in the gel at each time point was used to calculate the amount of protein released by difference. We assume that no protein is lost from HAMC during the period of release. To confirm the effect of denaturation on protein detectability by ELISA, known concentrations of EGF and PEG-EGF were boiled for 60 min in the presence of 2 mM β -mercaptoethanol. Detectability of thus treated proteins was compared to non-denatured proteins by ELISA. ELISA is a reliable method for detecting stable protein in tissue since proteins degraded or denatured are not detectable (Fig. S1). The concentrations in the homogenate were used to generate tissue penetration profiles for EGF and PEG-EGF as well as the protein mass balance at each time point.

2.8. Stability of EGF and PEG-EGF in proteases of the brain extracellular space

The stability of EGF and PEG-EGF were investigated in solutions of proteases extracted from the brain extracellular space (ECS). Extracellular enzymes were extracted as described previously by Shashoua et al. [23]. An extraction buffer of 0.32 M sucrose and 1 mM calcium acetate in dH₂O was first prepared. Uninjured and stroke-injured C57/BL6 mice were perfused with the extraction buffer. The brains were harvested and incubated on a rotary shaker (Orbitron Rotatr 1, Model # 260200, Boekel Scientific, Feasterville, PA, USA) in 25 ml of the extraction buffer for 2 h at 0 °C. The extract was concentrated using tubular protein concentrators (Ultracel 3 kDa MWCO UFC 900324, Millipore, Billerica, MA, USA) until the final volume was approximately 3 ml. The concentrate was then centrifuged at 16249 g for 90 min and the supernatant was dialysed in 3500 kDa MWCO dialysis cassettes (Slide-A-Lyzer 66330, Thermo Scientific, Rockford, IL, USA) against 150 mM PBS for 24 h. The total protein concentrations in both samples were estimated using a UV spectrophotometer (UV-vis ND-100, Nanodrop, Wilmington, DE, USA), and the solutions were diluted in PBS such that the total protein concentrations in all samples were equal.

The stability of EGF and PEG-EGF were determined in brain ECS samples over 48 h at 37 °C. 100 μ l of the incubating media was added to 1.5 ml eppendorf tubes and stored at 4 °C. At each time point, 5 μ l of 10 μ g/ml EGF or PEG-EGF solution was added to each extract and incubated at 37 °C. The time points examined were 0, 0.5, 1, 2, 3, 6, 8, 24 and 48 h. Immediately after the 0 h samples were taken, the stability of proteins in all samples were determined using EGF ELISA as per the manufacturer's instructions (PeproTech). The protein stability was compared to a sample in PBS incubated at 37 °C for the same period of time.

To verify that the mechanism of protein degradation is enzymatic proteolysis, a panel of protease inhibitor solutions was added to the ECS and homogenate solutions to inactivate the proteolytic enzymes present. The protease inhibitor panel was prepared with the following solution in dH₂O: 1 mM 4-(2-aminoethyl) benzene-sulfonyl fluoride hydrochloride (AEBSF), 1 mg/ml 6-aminohexanoic acid, 100 μ M antipain, 800 mM aprotinin, 4 mM benzamide HCl, 40 μ M bestatin, 100 μ M chymostatin, 10 μ M E-64, 1 mM N-ethylmaleimide, 100 μ M leupeptin, 1 μ g/ml pepstatin, 10 μ M phosphoramidon, and 10 mM trypsin inhibitor (INHIB1, Sigma–Aldrich). The protein stability assay was carried out as above and the ELISA detectable protein concentration was determined.

2.9. Effects of EGF and PEG-EGF released from HAMC on endogenous SVZ cell proliferation

Both uninjured and stroke-injured mice subjected to implantation surgeries of EGF or PEG-EGF were sacrificed 2 d following implantation and perfused with 10 ml saline followed by 10 ml 4% PFA. The brains were harvested and post-fixed in 4% PFA for 24 h at 4 °C, and subsequently cryoprotected with 20% sucrose solution for 24 h.

Brains were cryosectioned at 10 μ m and all tissue sections from Bregma 1.94 to Bregma –2.92 were collected. Sections were stained with the following antibodies: rabbit anti-mouse Ki67 (1:200); mouse anti-human Ki56 (1:200); mouse anti-rat nestin (1:200); rabbit anti-mouse DCX (1:200). With the following secondary antibodies: Alexa 568 goat IgG (1:200); Alexa 488 goat-anti-rabbit IgG (1:200); Alexa 564 goat-anti-rabbit IgG (1:200); Alexa 488 goat-anti-mouse IgG (1:200); Alexa 568 goat-anti-mouse IgG (1:200).

To determine the effect of EGF and PEG-EGF released from HAMC on endogenous SVZ cell proliferation, every 5th tissue section was stained and all Ki-67⁺/DAPI⁺ cells along the lateral walls of the ipsilateral and contralateral ventricles were counted. Additionally, ten random sections were selected from each uninjured and stroke-injured, PEG-EGF treated animals, and co-stained with Ki67 nestin or DCX. Double-positive cells along the SVZ were quantified as a percent of total Ki67⁺ cells.

2.10. Statistics

Data are presented as mean \pm standard deviation. Comparisons between multiple groups were conducted using one-way ANOVA with Bonferroni correction. Significance levels were indicated by $p < 0.05$ (*), 0.01 (**), and 0.001 (***)

3. Results

3.1. *In vitro* release of EGF from HAMC

The release of EGF and PEG-EGF from HAMC was first studied *in vitro* over 24 h (Fig. S2A). Approximately 80% of protein in HAMC was released within the first 8 h, and approximately 100% was released by 24 h. The release was diffusion controlled between 30 min and 8 h, as the fractional protein release was proportional to $t^{0.5}$ (Fig. S2B) [24]. Between 0 and 30 min, the release did not follow diffusion-controlled profile due to swelling of HAMC, which reached equilibrium after 30 min of incubation in buffer. Diffusional release of PEG-EGF from HAMC was not slower than EGF, despite the hydrodynamic radius of PEG-EGF being larger than that of EGF [25,26], indicating that the pore size of HAMC is greater than the hydrodynamic radius of PEG-EGF.

3.2. *In vivo* elimination of EGF and PEG-EGF in uninjured and stroke-injured animals

HAMC containing either EGF or PEG-EGF was implanted on top of both uninjured and stroke-injured mouse brains 4 days post stroke. *In vitro* EGF release data suggested that the majority of epicortical delivered EGF and PEG-EGF from HAMC were released

within 2 days. We therefore extracted the EGF and PEG-EGF remaining in HAMC on top of the brain at 2 h, 6 h, 1 d, and 2 d post-implantation and measured the amount present by ELISA. As predicted, the amount of protein remaining in HAMC decreased at each subsequent time point (Fig. 2A, B). Significant differences were neither found between EGF and PEG-EGF groups nor between injured and uninjured groups.

Similarly, to determine the elimination rate of delivered proteins, we measured detectable protein levels in brain tissues at 2 h, 6 h, 1 d, and 2 d. Proteins detected were normalized to the expected amount released at each time, as determined from the mass of protein detected in HAMC. PEG-EGF was eliminated at significantly slower rates than EGF from both uninjured (Fig. 2C) and stroke-injured brains (Fig. 2D). In uninjured brains, at 2 h post implant, 90% of the EGF and PEG-EGF released from HAMC was detected by ELISA. At 6 h, 1 d, and 2 d post implant, significantly more PEG-EGF was detectable in tissue compared to EGF ($p < 0.05$). Indeed, at 2 d post implant, only 10% of EGF was detected whereas 60% of PEG-EGF was found. Similarly, in stroke-injured brains, significantly more PEG-EGF was detected in tissue compared to EGF at all times examined. Even at 2 d post implant, the quantity of PEG-EGF significantly exceeded that of EGF though only low levels of both EGF and PEG-EGF were detected ($p < 0.05$).

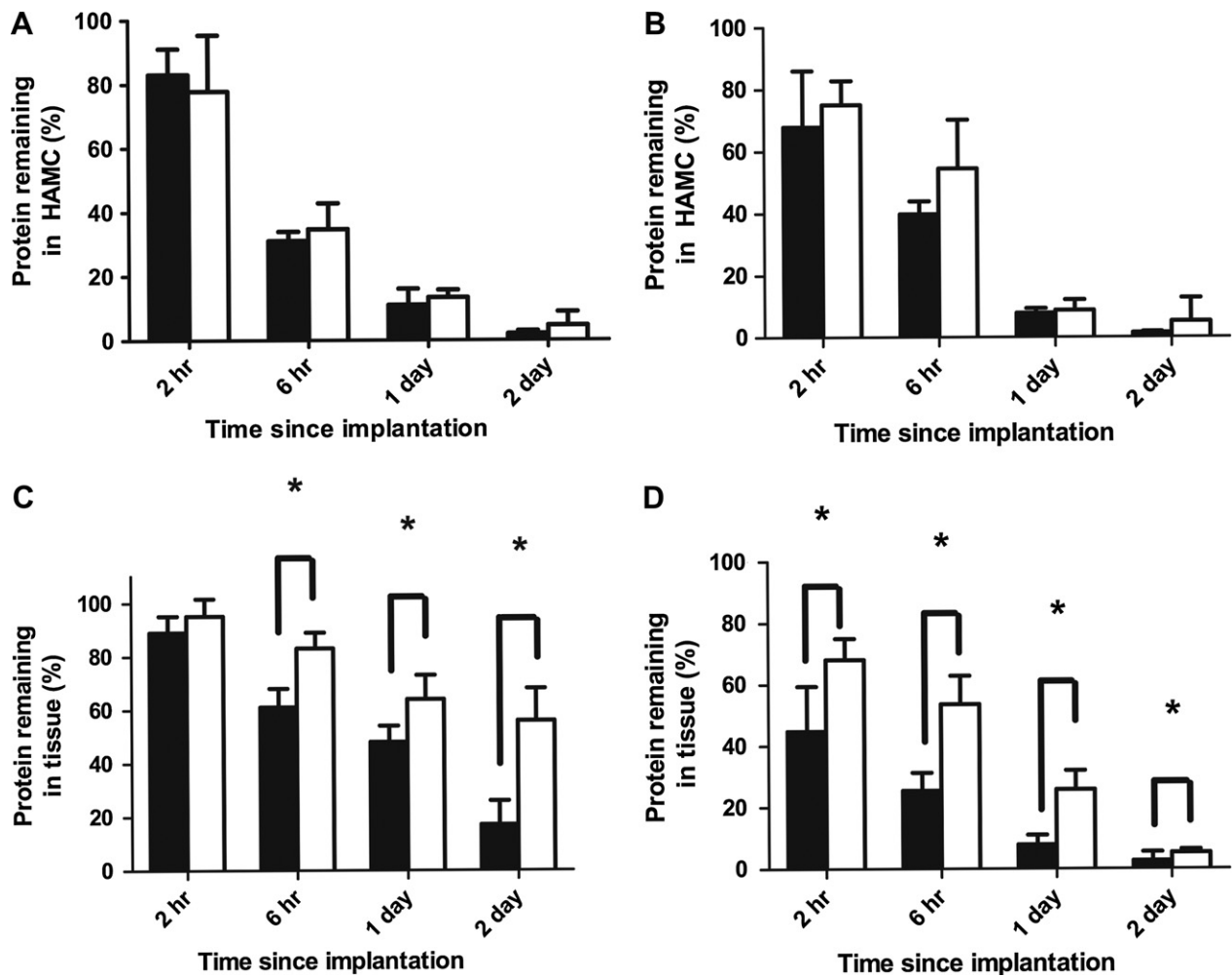


Fig. 2. PEG-modified EGF has slower rates of elimination compared to native EGF *in vivo*. The amount of (■) EGF and (□) PEG-EGF detected after 2 h, 6 h, 1 d and 2 d was quantified. (A) Quantification of the amount of protein remaining in HAMC normalized to starting mass in uninjured and (B) stroke-injured brains. (C) The amount of protein was first quantified in the brain tissue by ELISA, and this amount was then divided by the total amount of protein released from HAMC to determine mass percent in uninjured and (D) stroke-injured brains ($p < 0.05$, $n = 3$, mean \pm SD reported).

3.3. *In vivo* penetration profiles of EGF and PEG-EGF in uninjured and stroke-injured animals

Protein penetration in brain tissue is severely limited by rapid elimination [27]. Based on previous studies [21], it was hypothesized that PEG-modification of EGF would reduce rates of elimination, thereby allowing the protein to diffuse further. To this end we investigated the tissue penetration profiles of EGF and PEG-EGF at 2 h, 6 h, 1 d, and 2 d following release from HAMC in both uninjured and stroke-injured mice. Six 500 μm sequential tissue sections were prepared ventral to the cortical surface and the delivered proteins were extracted for analysis by ELISA.

In the uninjured brain, at 2 h post-implantation, the majority of protein was found between 0 and 500 μm below the cortical surface for both EGF and PEG-EGF (Fig. 3A). At 6 h post-implantation (Fig. 3B), the majority of EGF was found at depths between 0 and 1500 μm with trace amounts observed at 1500–2500 μm . Significantly higher concentrations of PEG-EGF were found at 1500–2500 μm compared to EGF at 6 h post implant ($p < 0.05$), while at 1 d post-implantation (Fig. 3C), the concentrations of PEG-EGF observed between 2500 and 3000 μm significantly exceeded that of EGF ($p < 0.05$). At 2 d post-implantation (Fig. 3D), the amounts of PEG-EGF found in all tissue sections exceeded that of EGF ($p < 0.05$), and there was at least a two-fold increase of protein accumulation due to PEG-modification. This suggests that EGF was cleared faster than PEG-EGF, and demonstrates

that PEG-EGF was able to penetrate deeper into uninjured brain tissue than unmodified EGF.

In stroke-injured brains, a similar trend was observed. At early times (Fig. 4A, B), the penetration profile of PEG-EGF resembled that of EGF. At 1 d post implant (Fig. 4C), PEG-EGF was observed throughout the 3000 μm of tissue analysed while the amounts of EGF found deeper than 1000–1500 μm are negligible. PEG-modification lead to a greater than seven-fold increase in protein accumulation. At 2 d post-implantation (Fig. 4D), while there was minimal EGF and PEG-EGF found in the deeper tissue slices, the protein accumulation achieved by PEG-modification was ten-fold greater between 500 and 2000 μm , and more than twenty-fold greater between 2000 and 3000 μm . This finding is promising for delivery to the NSPC niche in the SVZ, which is approximately 2000–3000 μm ventral to the cortical surface. While unmodified EGF may not be able to reach the SVZ in efficacious doses, PEG-EGF will likely reach the SVZ at sufficiently high doses, thereby stimulating NSPC proliferation *in vivo*.

3.4. *In vitro* proteolytic stability of EGF and PEG-EGF in brain extracellular space (ECS) and intracellular enzyme solutions

According to the tissue mass balance of delivered EGF and PEG-EGF, it is clear that PEG-EGF was eliminated more slowly than EGF. One of the major mechanisms of protein elimination in the brain is

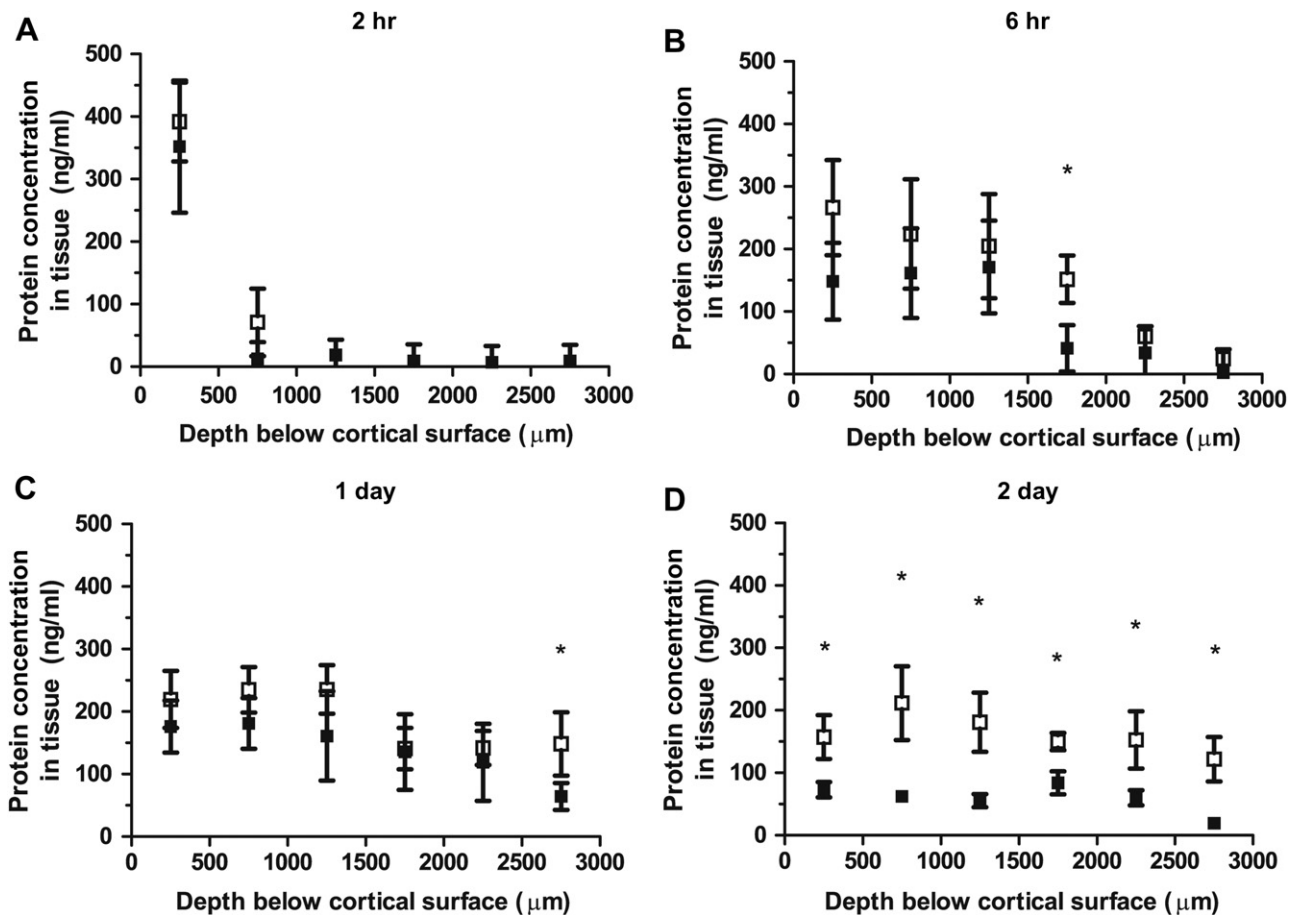


Fig. 3. PEG-modification of EGF allows for deeper tissue penetration in uninjured brains after delivery from implanted HAMC. Following implantation in uninjured mouse brains, the diffusion profiles of (■) EGF and (□) PEG-EGF at different depths is assessed. (A) At 2 h post-implantation protein concentration is similar. (B) At 6 h post-implantation, while significantly more PEG-EGF is found between 1500 and 2000 μm , the profiles remain similar in all other tissue sections. (C) 1 day post-implantation, significantly higher concentrations of PEG-EGF are found 2500–3000 μm below the cortical surface. (D) 2 days post-implantation, more PEG-EGF is found at all depths examined ($p < 0.05$, $n = 3$, mean SD reported).

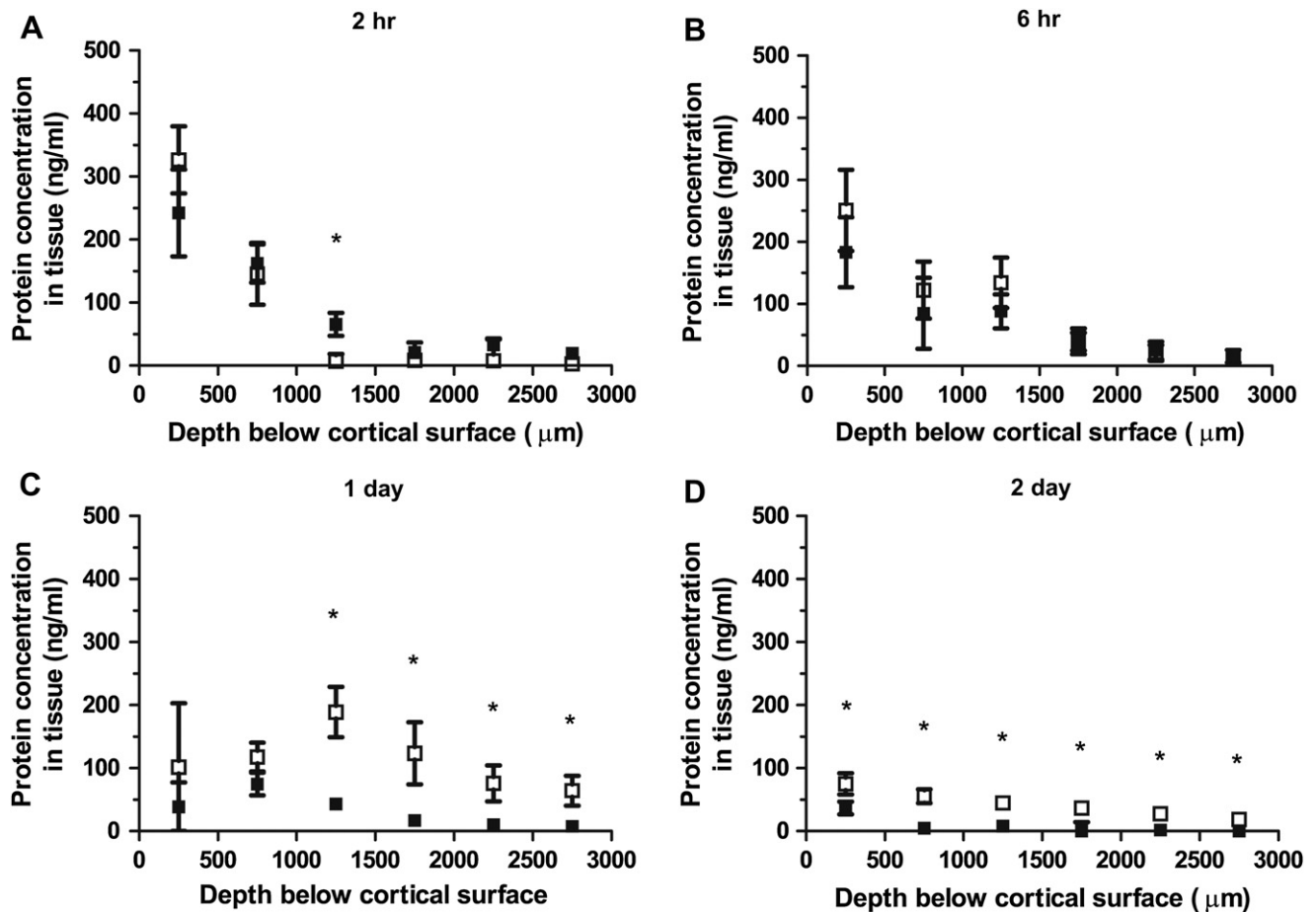


Fig. 4. PEG-modification of EGF allows for deeper tissue penetration in stroke-injured brains after delivery from implanted HAMC. Following implantation in stroke-injured mouse brains, the diffusion profiles of (■) EGF and (□) PEG-EGF at different depths is assessed. (A) At 2 h and (B) 6 h post-implantation diffusion profiles appear similar. (C) 1 day post-implantation, significantly more PEG-EGF is found between 1000 and 3000 μm (D) 2 days post-implantation, higher levels of PEG-EGF are found at all depths examined ($p < 0.05$, $n = 3$, mean SD reported).

enzymatic degradation [28]. To gain insight into this possible mechanism of degradation, we studied the stability of EGF and PEG-EGF in proteases extracted from the extracellular space of the brain *in vitro*. In protein extracts from uninjured brains, PEG-EGF exhibited significantly higher stability than EGF (Fig. 5A). The half-life ($t_{1/2}$) of PEG-EGF was 3.52 h while that of EGF was 0.74 h (Fig. 5B). In extracts from stroke-injured brains, a similar trend was observed in the extracellular protein extracts (Fig. 5C), and the $t_{1/2}$ of PEG-EGF and EGF were 3.85 and 1.69 h, respectively. To confirm that the observed effect on protein stability is due to proteolytic degradation, we examined EGF and PEG-EGF stability in both PBS and protein extracts from stroke-injured brains treated with a panel of protease inhibitors (Fig. 5A, C). The stability of both EGF and PEG-EGF remained at initial levels over 8 h when incubated with protease inhibitors, suggesting that the degradation of EGF observed was predominately enzyme-mediated.

3.5. Effect of EGF and PEG-EGF delivered from HAMC on SVZ stem cell proliferation

Immunohistochemical staining with Ki67 was used as a measure of SVZ proliferation [29]. To ensure that the Ki67⁺ cells was an accurate measure of NSPC proliferation, sections from both stroke-injured mice and stroke-injured mice treated with PEG-EGF were co-stained with Ki67 and the NSPC markers nestin and DCX [30].

Following epi-cortical implantation of EGF and PEG-EGF, we examined the proliferation of SVZ NSPCs to determine whether the protein reaching the SVZ is bioactive. Both uninjured and stroke-injured mice were sacrificed 2 d post-implantation. Coronal brain sections from all treatment groups were stained with Ki67 and DAPI and co-stained cells along the lateral ventricles were quantified (representative images of SVZ from the stroke-injured group, Fig. 6A–D, and the stroke-injured/PEG-EGF treated group, Fig. 6E–H, are shown). The total number of Ki67⁺ proliferating cells in the SVZ was quantified ipsilateral and contralateral to the implant.

In uninjured brains with and without blank HAMC implants, the total cell number was not significantly different between the ipsilateral and contralateral SVZ (Fig. 6I). We did not observe an increase in NSPC proliferation resulting from HAMC alone. When treated with EGF and PEG-EGF delivered from HAMC, the number of proliferating NSPCs ipsilateral to the implant significantly exceeded that from the HAMC implant alone ($p < 0.05$). There was no difference observed contralateral to the implant between any of the test groups. The ipsilateral cell count exceeded the contralateral cell count following either EGF or PEG-EGF treatment ($p < 0.05$). This suggests that within 2 d post implant, EGF delivered from the hydrogel delivery system preferentially reached the ipsilateral SVZ and thus enhanced stem cell proliferation. We observed no significant difference in cell proliferation between EGF and PEG-EGF treatments ipsilateral to the implant. This indicates that in

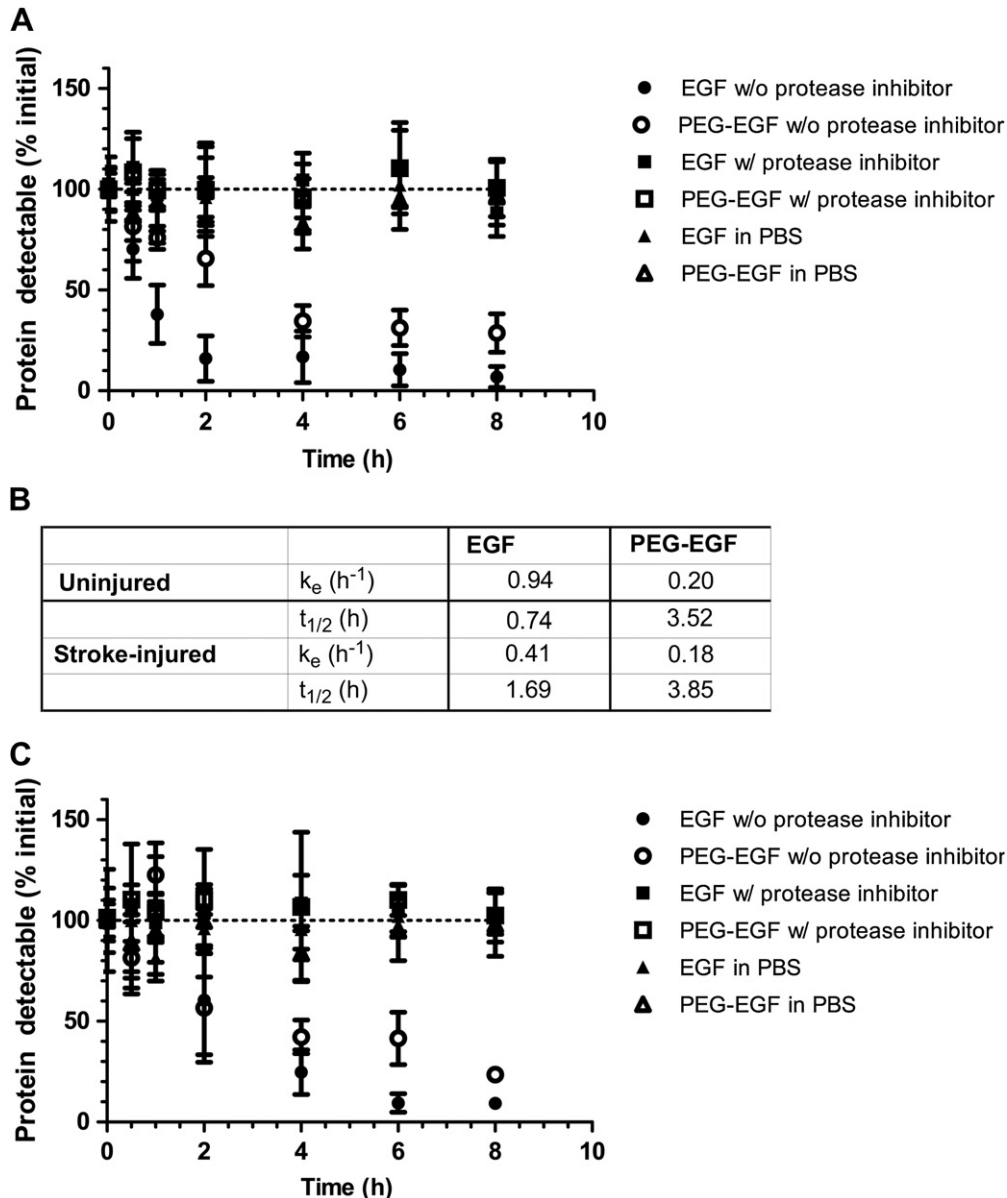


Fig. 5. PEG-EGF is more stable compared to native EGF in extracellular space proteins extracted from uninjured and injured brains. (A) In the uninjured brain, (○) PEG-EGF is degraded more slowly than (●) EGF in proteins extracted from the extracellular space. The stability of (▲) EGF and (△) PEG-EGF in PBS remained constant and similar to initial levels over time. The stability of (■) EGF and (□) PEG-EGF in protease inhibitor-treated ECS extract also remained constant. (B) The rates of degradation (k_e) and the half-lives ($t_{1/2}$) are quantified: PEG-EGF has a slower degradation rate than EGF in both uninjured and stroke-injured brains; and PEG-EGF has a longer half-life than EGF in both uninjured and stroke-injured brains. (C) PEG-EGF degrades more slowly than EGF in proteins extracted from the extracellular space of stroke-injured brains ($n = 3$, mean \pm SD reported).

uninjured brains, the dose of EGF reaching the SVZ is able to enhance NSPC proliferation, and the effect of EGF and PEG-EGF arriving at the SVZ within 2 d post implant is equivalent in terms of their ability to promote NSPC proliferation.

Stroke injuries increased the level of SVZ cell proliferation compared to uninjured controls, both ipsilateral and contralateral to the injury (Fig. 6j). Contralateral to stroke injuries, sham implants of aCSF and HAMC did not lead to differences in the proliferating cell population of the SVZ. There were no statistical differences between the EGF and PEG-EGF treated animals compared to control animals in the contralateral tissue. Ipsilateral to the stroke injuries, sham implants of aCSF and HAMC did not affect the number of proliferating SVZ cells compared to stroke surgeries alone. The total number of proliferating cells in the ipsilateral SVZ was significantly enhanced by both EGF ($p < 0.05$) and PEG-EGF ($p < 0.001$). PEG-EGF led to

higher numbers of proliferating cells ipsilateral to the implant compared to EGF ($p < 0.05$). This demonstrates that PEG-EGF was bioactive *in vivo*. It also demonstrates that PEG-EGF was more effective than EGF in stimulating NSPC proliferation in stroke-injured brains, when delivered using the minimally-invasive HAMC epi-cortical delivery vehicle. The effect of PEG-EGF was only observed in the SVZ ipsilateral to the implant, suggesting that epi-cortical delivery is able to target the ipsilateral tissue, thereby confining the effect to the desired region.

We confirmed that the factors delivered epi-cortical from HAMC were efficacious in terms of stimulating precursor cell populations in the SVZ. EGF is a known mitogen for precursor cells in the SVZ [30,31]. We determined that treatment with PEG-EGF led to more pronounced SVZ cell proliferation compared to baseline conditions. Therefore sections from stroke-injured mice treated with and

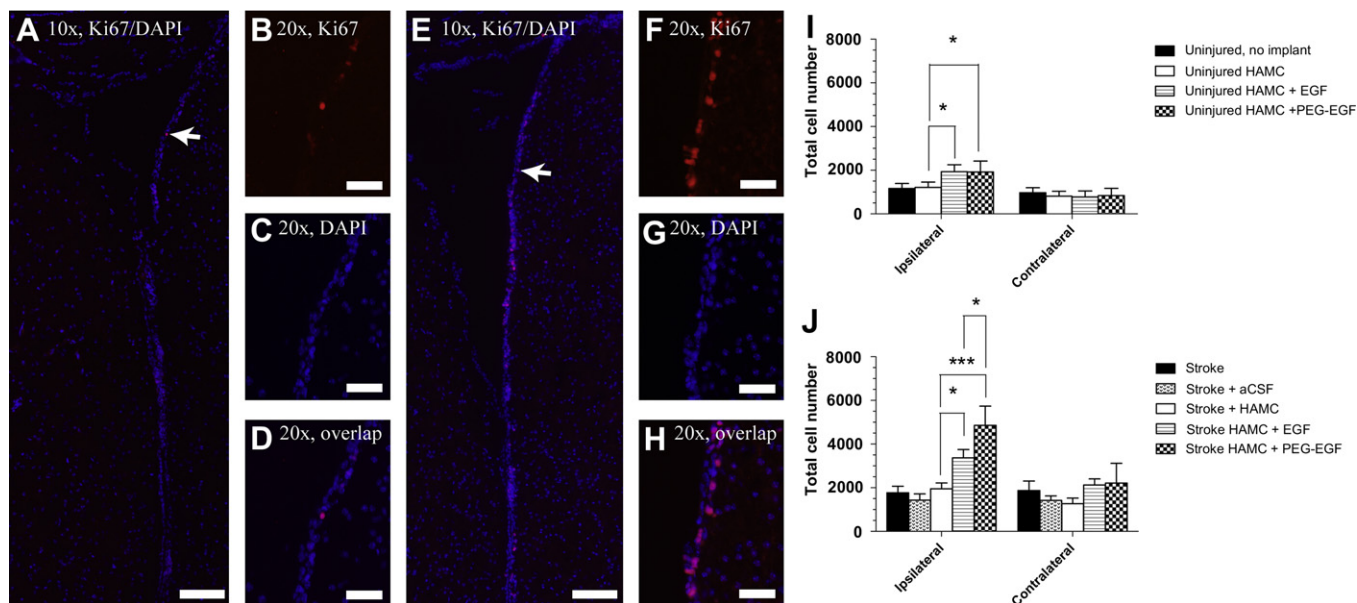


Fig. 6. When delivered epi-cortically from HAMC, PEG-EGF stimulates higher levels of subventricular zone cell proliferation compared to EGF. Uninjured and stroke-injured mice are treated with EGF and PEG-EGF delivered epi-cortically from HAMC. (A–D) Representative images are shown for Ki67 staining of stroke-injured and (E–H) stroke-injured/PEG-EGF treated groups. Arrows indicate double-labelled cells in the SVZ. (I) Quantification of Ki67 positive cells in uninjured brains show that both PEG-EGF and EGF increased SVZ cell proliferation by 1.6 fold compared to control groups ($p < 0.05$), while no significant difference was observed contralateral to the implant. (J) In stroke-injured brains EGF enhanced cell proliferation in the SVZ, compared to control groups ($p < 0.05$). PEG-EGF showed greater effect in increasing proliferation relative to both all control groups ($p < 0.001$) and EGF ($p < 0.05$). There were no significant differences among the groups contralateral to the implant ($n = 3$, mean \pm SD reported). A, E Scale: 100 μ m, B–D, F–H Scale: 40 μ m.

without PEG-EGF were double-stained with Ki67 and the NSPC marker nestin or the neuroblast marker DCX. We found that the number of Ki67⁺ cells that were double positive for DCX (Fig. 7A–C) to be significantly increased in PEG-EGF treated stroke-injured animals compared to the stroke-only animals ($p < 0.05$). More nestin⁺ Ki67⁺ cells appear to be upregulated in PEG-EGF treated stroke animals (Fig. 7D–F) than stroke-only animals; however, no statistical difference was observed. These results suggest that PEG-EGF stimulated the SVZ precursor cell populations.

4. Discussion

Here we investigated the potential of using HAMC as a local drug delivery vehicle for treating stroke. By placing HAMC remotely from the target site, we avoid risks of trauma and infection observed when inserting cannulae and needles into the brain tissue [32]. In our system, HAMC is delivered on top of the cortex, thereby minimizing tissue damage compared to systems where the reservoir is either directly inserted into the tissue [27,33] or a burr hole is drilled into the brain tissue to create a void for the reservoir [4].

One important factor impeding the use of polymeric drug delivery systems in the brain is short protein penetration distance. Previous studies have shown protein diffusion to be restricted to 1–2 mm in brain tissue [34], an inadequate distance for NSPC stimulation as the niche is deep within the brain. Our present study shows that by modifying EGF with PEG, we significantly increase the amount of protein accumulated 2–3 mm ventral to the cortical surface, 1–2 days after HAMC delivery. These distances exceed previously reported distances of protein diffusion in the uninjured brain and correspond to the depth of the SVZ [35,36]. These features demonstrate that HAMC is a suitable candidate for localized sustained drug delivery to the brain, yet we recognize that 3 mm of tissue penetration is adequate in mouse models, but may be inadequate in humans to stimulate SVZ precursor cells.

PEG-modification resulted in a 3-fold increase in EGF penetration distance in the uninjured brain and up to 27-fold increase in

stroke-injured brain. The benefit of PEG-modification is amplified in the stroke-injured brain. We have previously demonstrated that following stroke there is an upregulation of EGFR [21]. This increase in receptors post stroke will increase the rate of elimination and could account for the increased efficacy of PEGylation in stroke-injured animals when compared to uninjured animals.

We propose that the increased penetration distance of PEG-EGF can be further enhanced through the use of a constant protein source. We [37] and others [27,34] previously showed that proteins released from a constant source will increase diffusion in the brain by 2-fold compared to a single injection. Proteins encapsulated in poly(lactide-co-glycolide) micro/nanospheres and incorporated into HAMC can be used to achieve a range of delivery periods, between 7 and 30 days [37]. This type of long-term sustained delivery device will provide the constant source required to further increase protein diffusion distance in the brain. By releasing growth factors close to the target sites, the amount of protein required will be reduced as will the volume of tissue exposed, thereby decreasing the risk of tumour development associated with long-term growth factor delivery.

We studied the stability of EGF and PEG-EGF during diffusion by examining their rates of degradation in brain-extracted solutions. PEG-modification of EGF improved EGF stability and corroborates previously reported results, where PEG improved the stability of various proteins *in vitro* [38]. We found both EGF and PEG-EGF to be eliminated faster in stroke-injured brains compared to uninjured brains. This is likely due to activation of inflammatory cells and over-expression of proteolytic enzymes [28].

The observation that stroke injuries increase cell proliferation in the SVZ is consistent with previous findings [39]. The effect of injury alone, however, does not adequately enhance proliferation and tissue regeneration. Significantly greater total numbers of proliferating cells in uninjured brains are observed after EGF or PEG-EGF treatment, than untreated controls. This demonstrates the benefit of remote delivery and also suggests that the amounts of both EGF and PEG-EGF that reach the SVZ may saturate the EGFR.

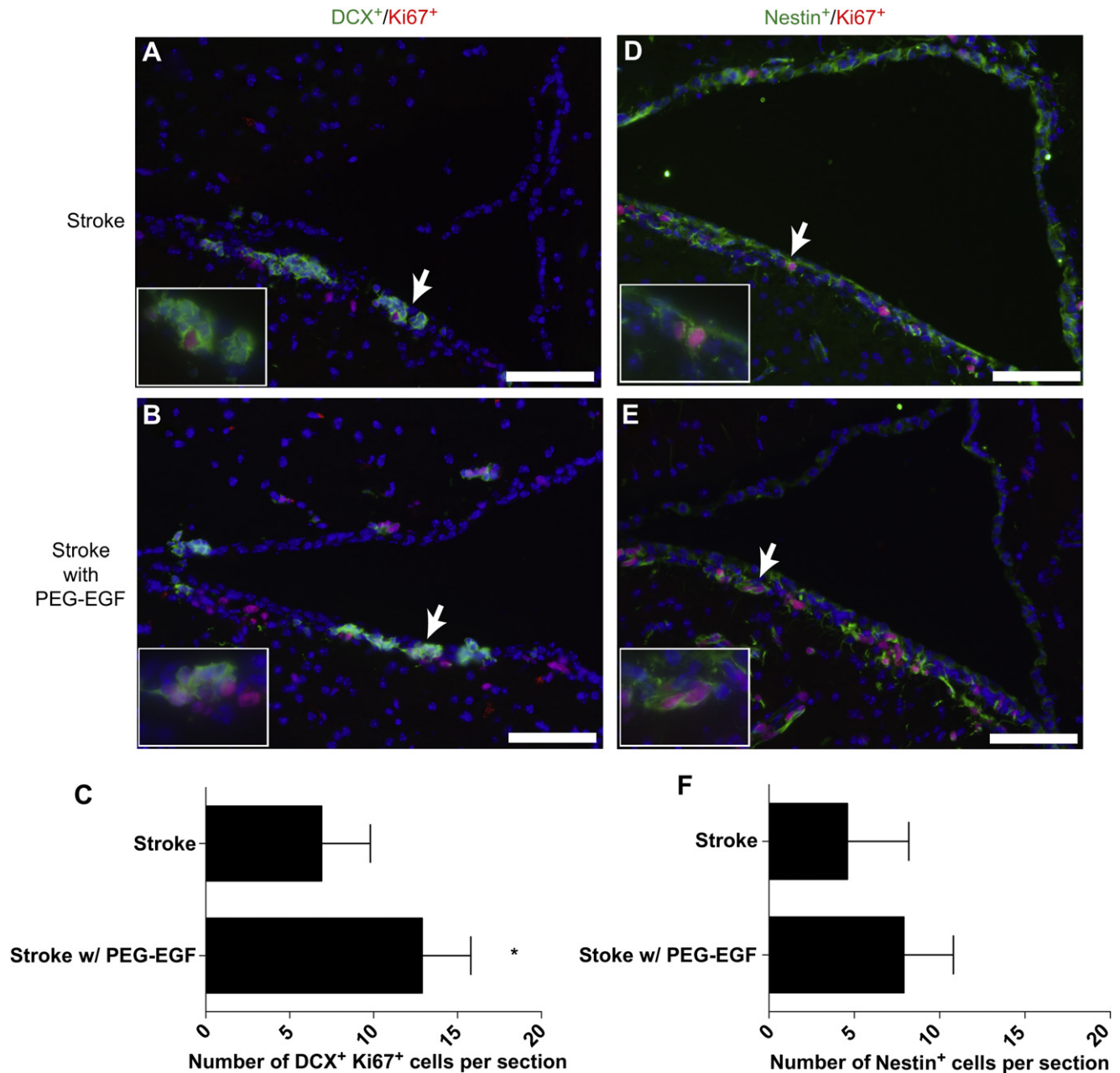


Fig. 7. Proliferating precursor cell populations in the SVZ. Sections from stroke-injured and stroke-injured/PEG-EGF treated brains are stained with Ki67 and one of either double-cortin (DCX) or nestin. (A) stroke-injured and (B) stroke-injured/PEG-EGF treated brains co-stained with DCX and Ki67. (C) Quantification of cells double-stained with Ki67 and DCX. (D) stroke-injured and (E) stroke-injured/PEG-EGF treated brains co-stained with nestin and Ki67. (F) Quantification of cells double-stained with Ki67 and nestin. Significant difference was found between stroke-injured and stroke-injured/PEG-EGF treated groups for DCX⁺ Ki67⁺ ($p < 0.05$, $n = 3$, mean \pm SD reported). Images were taken at 20 \times magnification. Insets show arrow-indicated regions at 60 \times magnification. Scale: 100 μ m.

Significantly, the results reported herein have broad applicability to other areas of controlled molecule delivery to the brain. For example, our system could be used to deliver a myriad of clinically relevant agents, including small molecule drugs [40], protein therapeutics [7], and imaging agents [41].

5. Conclusions

Our results demonstrate the potential of HAMC as a drug delivery vehicle for local release to the brain and the use of PEG as a modifier to enhance protein stability, diffusion distance, and *in vivo* bioactivity. We demonstrate that injection of HAMC on the brain cortex achieves direct delivery to the brain tissue, obviating the need to

cross the BBB or use minipump/catheter systems. PEG-EGF enhances NSPC proliferation in both uninjured and stroke-injured brains with the greatest number of NSPCs stimulated ipsilateral to the stroke injury with PEG-EGF delivery. This delivery system is beneficial because it achieves local delivery to the brain in a minimally-invasive way, and may enable the clinical translation of minimally-invasive epi-cortical drug delivery strategies.

Author contributions and declarations

M.J.C. – concept and design, performed all surgeries, collection of immunohistochemistry data, data analysis and interpretation; Y.W. – concept and design, collection and assembly of all data, data

analysis and interpretation; C.M.M – concept and design, data interpretation; M.S.S. – concept and design, data analysis and interpretation. All authors contributed towards preparation and final approval of manuscript.

The authors declare no competing financial interests.

Acknowledgements

We thank Dr. Douglas Baumann for intellectual discussions on the design of *in vitro* hydrogel swelling/drug release experiment. We acknowledge funding from the Heart and Stroke Foundation (CMM, MSS), the Natural Science and Engineering Research Council (YW), the Ontario Neurotrauma Foundation (MJC), and the Canadian Institute of Health Research (MSS). Authors M.J.C. and Y.W. contributed equally to this work.

Appendix. Supplementary material

Supplementary data related to this article can be found online at doi:10.1016/j.biomaterials.2011.04.032.

References

- Jablonska B, Gierdalski M, Kublik A, Skangiel-Kramska J, Kossut M. Effects of implantation of alzet 1007d osmotic minipumps upon 2-deoxyglucose uptake in the cerebral cortex of mice. *Acta Neurobiol Exp* 1993;53:577–80.
- Bear MF, Kleinschmidt A, Gu Q, Singer W. Disruption of experience-dependent synaptic modifications in striate cortex by infusion of an nmda receptor antagonist. *J Neurosci* 1990;10(3):909–25.
- Paradiso MA, Bear MF, Daniels JD. Effects of intracortical infusion of 6-hydroxydopamine on the response of kitten visual-cortex to monocular deprivation. *Exp Brain Res* 1983;51(3):413–22.
- de Boer AG, Gaillard PJ. Strategies to improve drug delivery across the blood-brain barrier. *Clin Pharmacokinet* 2007;46(7):553–76.
- Nave KA, Probstmeier R, Schachner M. Epidermal growth-factor does not cross the blood-brain-barrier. *Cell Tissue Res* 1985;241(2):453–7.
- Ford GA, Bryant CA, Mangoni AA, Jackson SHD. Stroke, dementia, and drug delivery. *Brit J Clin Pharmacol* 2004;57(1):15–26.
- Kolb B, Morshead C, Gonzalez C, Kim M, Gregg C, Shingo T, et al. Growth factor-stimulated generation of new cortical tissue and functional recovery after stroke damage to the motor cortex of rats. *J Cerebr Blood F Metab* 2007;27(5):983–97.
- Erlundsson A, Lin A, Yu F, Morshead CM. Immunosuppression promotes endogenous neural stem and progenitor cell migration and tissue regeneration after ischemic injury. *Exp Neurol*, in press.
- Doetsch F, Caille I, Lim DA, Garcia-Verdugo JM, Alvarez-Buylla A. Subventricular zone astrocytes are neural stem cells in the adult mammalian brain. *Cell* 1999;97(6):703–16.
- Salman H, Ghosh P, Kernie SG. Subventricular Zone Neural Stem Cells Remodel the Brain following Traumatic Injury in Adult Mice. *J Neurotrauma* 2004;21(3):283–92.
- Riquelme PA, Drapeau E, Doetsch F. Brain micro-ecologies: neural stem cell niches in the adult mammalian brain. *Philos T R Soc B* 2008;363(1489):123–37.
- Jin KL, Wang XM, Xie L, Mao XO, Zhu W, Wang Y, et al. Evidence for stroke-induced neurogenesis in the human brain. *Proc Natl Acad Sci USA* 2006;103(35):13198–202.
- Marti-Fabregas J, Romaguera-Ros M, Gomez-Pinedo U, Martinez-Ramirez S, Jimenez-Xarrie E, Marin R, et al. Proliferation in the human ipsilateral subventricular zone after ischemic stroke. *Neurology* 2010;74(5):357–65.
- Teramoto T, Qu JH, Plumier JC, Moskowitz MA. Egf amplifies the replacement of parvalbumin-expressing striatal interneurons after ischemia. *J Clin Invest* 2003;111(8):1125–32.
- Kalluri HSG, Dempsey RJ. Growth factors, stem cells, and stroke. *Neurosurg Focus* 2008;24(3–4).
- Sprigg N, Bath PMW. Colony stimulating factors (blood growth factors) are promising but unproven for treating stroke. *Stroke* 2007;38(6):1997–8.
- Gupta D, Tator CH, Shoichet MS. Fast-gelling injectable blend of hyaluronan and methylcellulose for intrathecal, localized delivery to the injured spinal cord. *Biomaterials* 2006;27(11):2370–9.
- Kang CE, Tator CH, Shoichet MS. Poly(ethylene glycol) modification enhances penetration of fibroblast growth factor 2 to injured spinal cord tissue from an intrathecal delivery system. *J Controlled Release* 2010;144(1):25–31.
- Nicholson C. Diffusion and related transport mechanisms in brain tissue. *Rep Prog Phys* 2001;64(7):815–84.
- Franklin KBJ, Paxinos G. The mouse brain in stereotaxic coordinates. 3 ed. Academic Press; 2008.
- Wang Y, Cooke MJ, Lapitsky Y, Wylie RG, Sachewsky N, Corbett D, et al. Transport of epidermal growth factor in the stroke-injured brain. *J Control Release* 2011;149(3):225–35.
- Tennant KA, Jones TA. Sensorimotor behavioral effects of endothelin-1 induced small cortical infarcts in c57bl/6 mice. *J Neurosci Method* 2009;181(1):18–26.
- Shashoua VE, Hesse GW, Moore BW. Proteins of the brain extracellular fluid - evidence for release of s-100 protein. *J Neurochem* 1984;42(6):1536–41.
- Lin M, Meng S, Zhong W, Li ZL, Du QG, Tomasik P. Novel biodegradable blend matrices for controlled drug release. *J Pharm Sci* 2008;97(10):4240–8.
- Bailon P, Berthold W. Polyethylene glycol-conjugated pharmaceutical proteins. *Pharm Sci Technol Today* 1998;1(8):352–6.
- Fee CJ, Van Alstine JA. Peg-proteins: reaction engineering and separation issues. *Chem Eng Sci* 2006;61(3):924–39.
- Saltzman WM, Radomsky ML. Drugs released from polymers - diffusion and elimination in brain-tissue. *Chem Eng Sci* 1991;46(10):2429–44.
- Lo EH, Wang XY, Cuzner ML. Extracellular proteolysis in brain injury and inflammation: role for plasminogen activators and matrix metalloproteinases. *J Neurosci Res* 2002;69(1):1–9.
- Enwere E, Shingo T, Gregg C, Fujikawa H, Ohta H, Weiss S. Aging results in reduced epidermal growth factor receptor signaling, diminished olfactory neurogenesis, and deficits in fine olfactory discrimination. *J Neurosci* 2004;24(38):8354–65.
- Bouab M, Paliouras G, Aumont A, Forest-Bérard K, Fernandes KJ. Aging of the subventricular zone neural stem cell niche: evidence for quiescence-associated changes between early and mid-adulthood. *J Neurosci* 2010;173(26):135–49.
- Doetsch F, Petreanu L, Caille I, Garcia-Verdugo JM, Alvarez-Buylla A. Egf converts transit-amplifying neurogenic precursors in the adult brain into multipotent stem cells. *Neuron* 2002;36(6):1021–34.
- Hawrylyuk GWJ, Rowland J, Kwon BK, Fehlings MG. Protection and repair of the injured spinal cord: a review of completed, ongoing, and planned clinical trials for acute spinal cord injury. *Neurosurg Focus* 2008;25(5):E14.
- Saltzman WM. Biomaterials for drug delivery to the brain. *Protein Eng* 1997;10(1):78–83.
- Saltzman WM, Mak MW, Mahoney MJ, Duenas ET, Cleland JL. Intracranial delivery of recombinant nerve growth factor: release kinetics and protein distribution for three delivery systems. *Pharmaceut Res* 1999;16(2):232–40.
- Krewson CE, Saltzman WM. Transport and elimination of recombinant human ngf during long-term delivery to the brain. *Brain Res* 1996;727(1–2):169–81.
- Mahoney MJ, Saltzman WM. Millimeter-scale positioning of a nerve-growth-factor source and biological activity in the brain. *Proc Natl Acad Sci USA* 1999;96(8):4536–9.
- Baumann MD, Kang CE, Stanwick JC, Wang YF, Kim H, Lapitsky Y, et al. An injectable drug delivery platform for sustained combination therapy. *J Control Release* 2009;138(3):205–13.
- Novaes LCD, Mazzola PG, Pessoa A, Penna TCV. Effect of polyethylene glycol on the thermal stability of green fluorescent protein. *Biotechnol Prog* 2010;26(1):252–6.
- Felling RJ, Levison SW. Enhanced neurogenesis following stroke. *J Neurosci Res* 2003;73(3):277–83.
- Bakhshi S, North RB. Implantable pumps for drug delivery to the brain. *J Neuro-Oncol* 1995;26(2):133–9.
- Heiss JD, Walbridge S, Asthagiri AR, Lonser RR. Image-guided convection-enhanced delivery of muscimol to the primate brain laboratory investigation. *J Neurosurg* 2010;112(4):790–5.